

# Growth regimes of CdTe deposited by close-spaced sublimation for application in thin film solar cells

J. Luschitz, K. Lakus-Wollny, A. Klein, W. Jaegermann \*

*Darmstadt University of Technology, Institute of Materials Science, Petersenstrasse 23, 64287 Darmstadt, Germany*

Available online 19 December 2006

## Abstract

We have systematically investigated the growth of CdTe thin films by Close Spaced Sublimation (CSS). Thin films of CdTe were deposited onto CdS substrates held at temperatures in the range 250 to 550 °C. The effect of substrate temperature and evaporation rate on structure and surface morphology of CdTe films were investigated. Up to 450 °C substrate temperature the growth rate was almost constant and decreased exponentially for higher temperatures. The structures of the CdTe films were determined by XRD and a strong (111) orientation was observed within the temperature range 250 °C–470 °C. Above 470 °C the texture changed to mostly (311) and (220) orientations. Surface morphology and grain size of CdTe growth was determined with AFM and SEM. The morphology of the layers showed three major modes: Columnar grains with a diameter of 0.2 µm and a length of 6 µm for temperatures from 250 °C to 350 °C, pyramidal grains with a diameter of 0.5–1.5 µm up to 470 °C and irregular shaped grains with a diameter of 5–10 µm for temperatures up to 550 °C. The roughness increased linearly from 15 nm to 220 nm within the substrate temperature range.

© 2007 Elsevier B.V. All rights reserved.

**Keywords:** Cadmium telluride; Growth mechanism; Scanning electron microscopy; X-ray diffraction

## 1. Introduction

CdTe in thin film photovoltaic applications promises to be a low cost alternative to common silicon technology. However, the highest reached conversion efficiency is 16.5% for laboratory solar cells [1] and only 8–10% for commercial photovoltaic modules and therefore much lower than the theoretical limit of 29.7% [2]. Due to the high absorption coefficient of CdTe [3], a film thickness of 2 µm should be sufficient to absorb most of the solar spectrum. In principle, a lower film thickness of the CdTe layer is favourable because of faster production and lower materials use. In addition, due to the low conductivity of the CSS–CdTe layers [4], a lower film thickness should result in a lower series resistance and therefore lead to a higher fill factor FF. However, thinner films have a higher probability for pinholes and shunts which could considerably reduce production yield on large area devices. In order to approach thin, pinhole-free CdTe layers, an enhanced

understanding in growth mechanisms is needed to control the morphology of the layers by suitable deposition conditions.

The influence of the deposition parameters on CdTe-film growth were studied by several groups. Lee [5] found an improvement in texture and electrical properties for increasing substrate temperatures in the very low temperature region (150–300 °C). Alamri [6] investigated the correlation between substrate temperature and growth rate, texture and morphology. In a recent work of Falcão [7] the influence of pressure, source and substrate temperature on CdTe morphology and structure were studied. We have systematically investigated the growth of CdTe thin films by Close Spaced Sublimation (CSS) using our dedicated system DAISY-SOL. The overall setup of the system is described in [8].

## 2. Experimental

The preparation of the CdS and CdTe-layers was performed in the Darmstadt Integrated SYstem for SOLar cell research (DAISY-SOL), a unique all-in-vacuum CSS-deposition system [8]. The CSS-unit consists of a moveable source and substrate,

\* Corresponding author. Tel.: +49 6151/16 6304; fax: +49 6151/16 6308.

E-mail address: [jaegerw@surface.tu-darmstadt.de](mailto:jaegerw@surface.tu-darmstadt.de) (W. Jaegermann).

which can be heated independently. This allows to simulate a dynamic and near industrial processing of solar cells. As in a commercial in-line process, the sample may be heated up almost independently before deposition, then moved above the source and moved away from the source after deposition for cooling down. Fig. 1 shows a photograph and a schematic drawing of the CdTe–CSS-unit (the CdS–CSS-unit is identical). Source and substrate are heated by halogen lamps. With the current setup, the sample temperature was not controlled during the deposition cycle but rather heated with a constant power during the experiments. As a consequence the sample temperature was rising exponentially while it was moved above the source. The increase in temperature was  $\sim 80$  °C within the first 50 s of deposition and 110 to 150 °C after 5 min, depending on whether the initial temperature is high or low. All sample temperatures given hereafter refer to the maximum temperature at the end of each deposition. The source temperature was measured by thermocouples.

The used substrate material was  $20 \times 20 \times 2$  mm borosilicate glass (SCHOTT BOROFLOAT® 33) covered with 250 nm sputtered ITO and 45 nm undoped  $\text{SnO}_2$  as a diffusion barrier. The substrates were cleaned in an ultrasonic bath with 2-propanol and deionised water.

To reduce the numbers of deposition parameters identical CdS-layer were deposited by CSS at a temperature of 515 °C for 2 min, resulting in a layer thickness of 180 nm and an average grain size of 200 nm. After cooling to 100–200 °C the samples were transferred into the CdTe–CSS-unit. The deposition process was performed as follows: 1.) heating up the sample

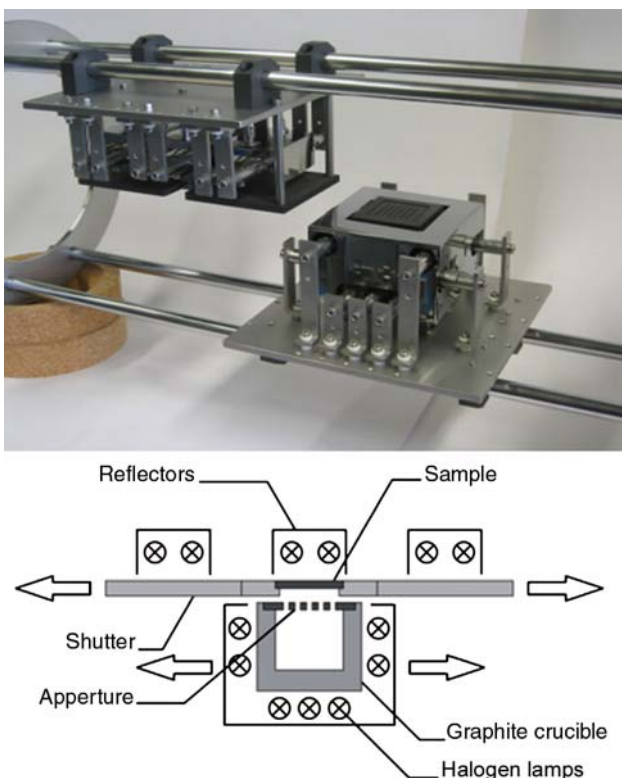


Fig. 1. CSS-deposition unit (+schematic).

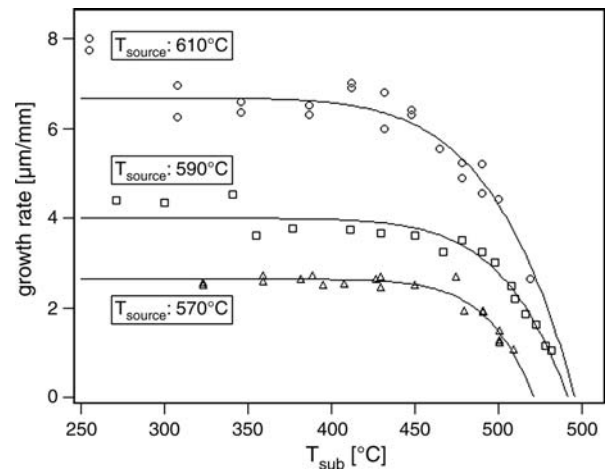


Fig. 2. Growth rate vs. substrate temperature for different source temperatures.

and source independently to the desired temperatures, 2.) moving the sample above the crucible and then starting the deposition, 3.) finally moving the sample away from the crucible and switching off the power supply for cooling down the sample and source. The transfer time in step 2) and 3) was  $\sim 5$  s, the deposition time varied from 30 s up to 5 min.

To investigate effects on CdTe-morphology the substrate temperature was varied from 250 to 550 °C which showed up to be the maximum temperature tolerated by the substrate glass as specified by the manufacturer and independently found by our own experience. Additionally, source temperatures of 570, 590 and 610 °C were used in order to investigate the effect of the CdTe vapour pressure. As the filling of the crucible was

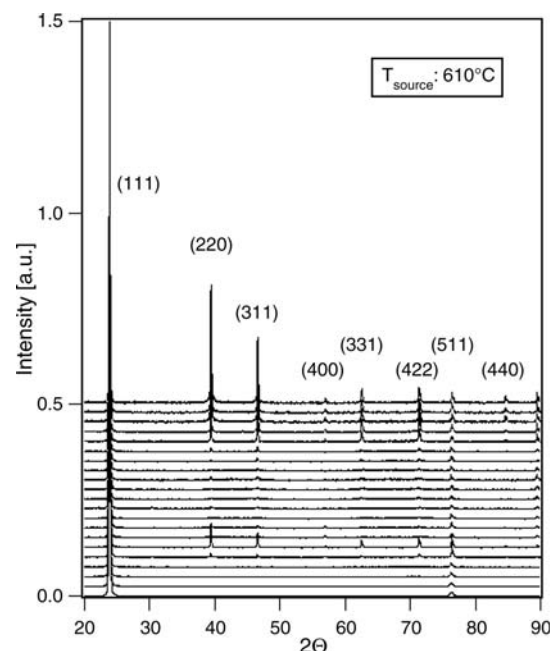


Fig. 3. Normalized XRD-patterns for a source temperature of 610 °C. The substrate temperature increases from bottom to top. The indices correspond to the (F4 $\bar{3}$ m) structure of CdTe.

decreasing with increasing number of experiments the source temperature was adjusted to maintain the nominal vapour pressure as it was measured for a maximum filling. To get comparable results all layers were deposited with similar thicknesses of 5–6  $\mu\text{m}$  as typically used for industrially produced layers. Therefore, for a given source temperature the deposition time had to be accordingly adjusted.

Afterwards all samples were measured with X-ray diffraction (XRD) and scanning electron microscopy (SEM) to study their structure and morphology.

### 3. Results

For each sample the growth rate was experimentally determined and calculated. The results are plotted in Fig. 2. For a source temperature of  $T_{\text{source}} = 590^\circ\text{C}$ , a drop of growth rate is observed at a substrate temperature of  $350^\circ\text{C}$ . This is most likely attributed to an incorrect adjustment of the source temperature to the filling of the crucible. The rather large scattering in growth rate for  $T_{\text{source}} = 610^\circ\text{C}$  is due to the very short deposition times. As already observed by Alamri [6], the growth rate can be distinguished into two regions. For substrate temperatures up to an extended breaking point the growth rate appears constant and depends only on the source temperature. For higher temperatures the growth rate is exponentially decreasing to zero, which is explained by increased re-evaporation of CdTe.

To investigate changes in texture, all samples were measured with XRD. Normalized patterns for a source temperature of  $610^\circ\text{C}$  are shown in Fig. 3. Experiments for other source temperatures gave similar results. For low substrate temperature a strong texture along the (111) direction is observed. For higher temperature the orientation of the grains becomes more random. To gain a more detailed view on layer

texture, texture coefficients  $C_i$  were calculated according to Harris analysis (1) [9]:

$$C_i = \frac{I_i/I_{0i}}{(1/N) \sum_{i=1}^N I_i/I_{0i}} \quad (1)$$

In Eq. (1)  $I_i$  is the intensity of the observed diffraction peak,  $I_{0i}$  the intensity of the same peak for a randomly orientated powder sample.  $N$  determines the number of considered reflections. A  $C$ -value of unity can then be interpreted as randomly oriented grains.

The results for the (111), (220), (331) and (422)-diffraction peaks are shown in Fig. 4. Up to a substrate temperature of  $\sim 460^\circ\text{C}$  a very strong (111) texture is observed. For higher temperatures the degree of texture drops to a near statistical value. For temperatures above  $520^\circ\text{C}$  the preferred orientation changes from (111) to a mixed (220) and (311) (not shown) distribution of grains. Interestingly, a drop in the (111)-texture coefficient is observed at a substrate temperature of  $\sim 350^\circ\text{C}$ , which is increasing again almost to its maximum value with further increase of substrate temperature.

Because of this observation three different regimes of texture are identified. The first regime for temperatures below  $350^\circ\text{C}$ , where only (111) and (333) (with same  $d$ -value as (511)) orientation is observed. The second regime reaches from temperatures from  $350^\circ\text{C}$  up to  $460^\circ\text{C}$ . It is characterized by an initial strong drop of (111)-texture and increase of intensities of all other reflections. The (111)-texture then recovers close to its previous value with all other diffraction peaks almost disappearing. Orientations perpendicular to the (111) direction ((220), (422)) show a significant line broadening which may be related to stresses along the CdS/CdTe-interface because of the lattice mismatch. The FWHM-value of these reflections slightly decreases for higher temperatures.

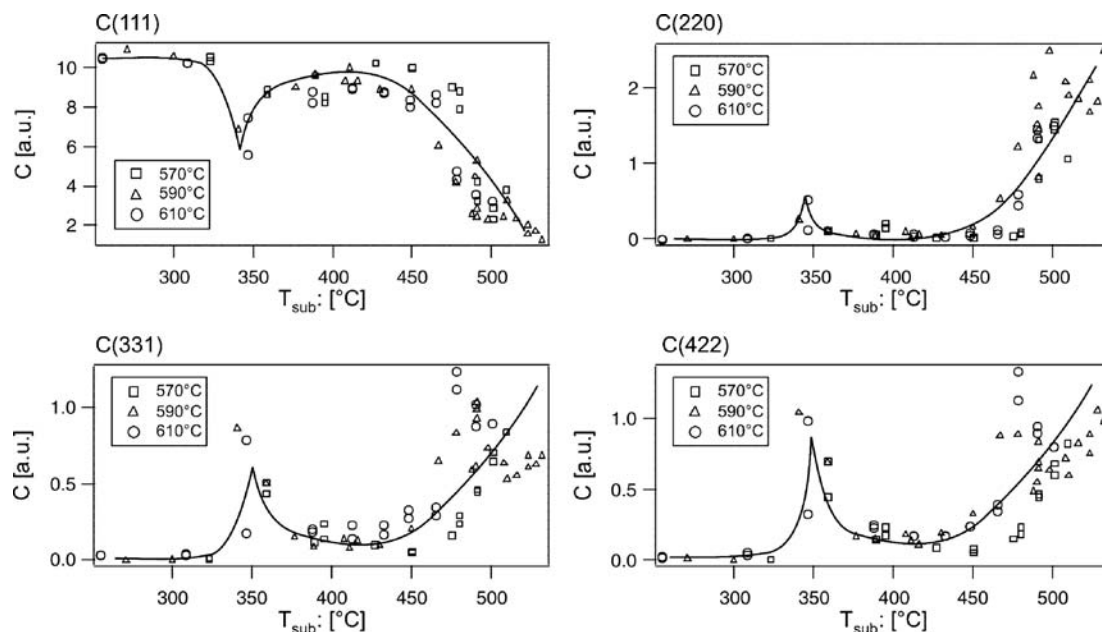


Fig. 4. Texture coefficients vs. substrate temperature for different source temperatures. Lines indicate the general behaviour as guide to the eye.



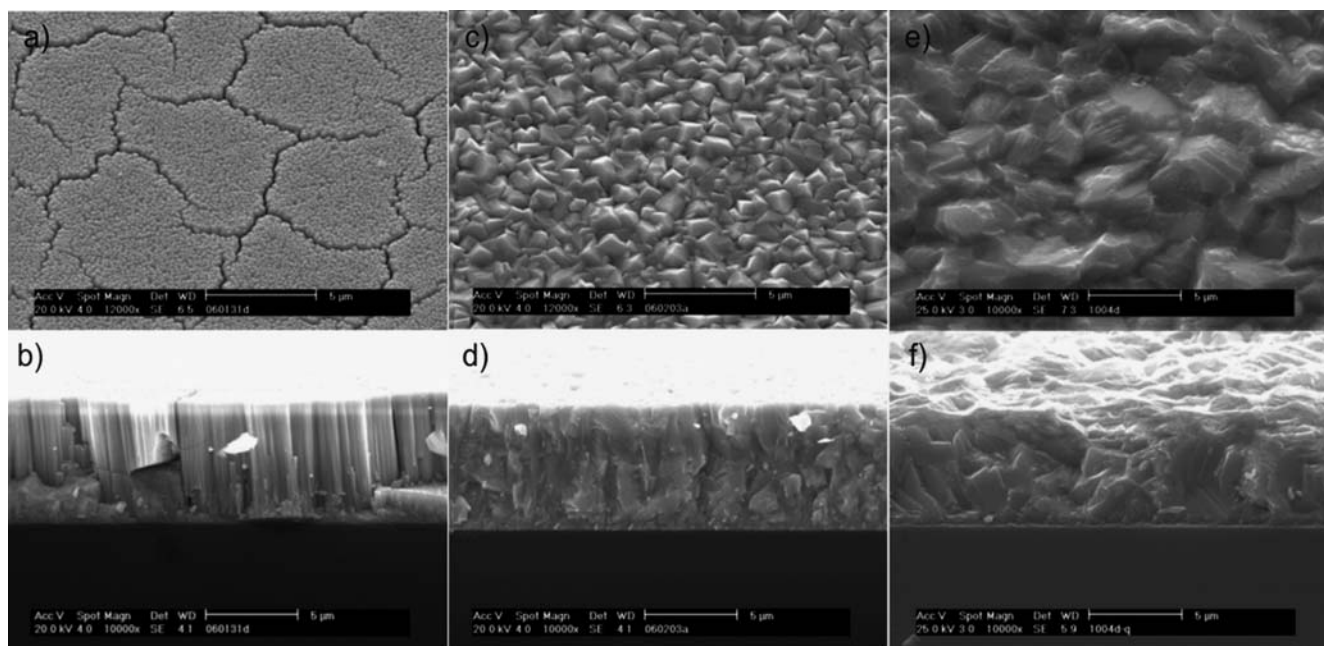


Fig. 5. SEM micrographs (surfaces and cross-sections) from the three growth regimes. a)+b) first regime ( $T_{\text{sub}}=255\text{ }^{\circ}\text{C}$ ), c)+d) second regime ( $T_{\text{sub}}=387\text{ }^{\circ}\text{C}$ ), e)+f) third regime ( $T_{\text{sub}}=523\text{ }^{\circ}\text{C}$ ). The scale bar represents  $5\text{ }\mu\text{m}$ .

The third regime is for temperatures above  $460\text{ }^{\circ}\text{C}$  and shows a complete disappearance of (111) texture to a near statistical orientation with slightly (220) and (311) preferred grain growth. The low temperature boundary of this last regime coincides with the onset of decreasing growth rate. According to Fig. 4, it appears that the temperature ranges of the three regimes do not depend on source temperature but only on substrate temperature. However, this might also be different for strongly different source temperatures, which, so far, have not been investigated.

All samples were studied with SEM to investigate changes in grain shape and size. Similar to the observation from XRD three major growth modes can be distinguished. The first mode results from the lowest achievable temperature ( $\sim 250\text{ }^{\circ}\text{C}$ ) to  $350\text{ }^{\circ}\text{C}$  and is characterized by strictly columnar grain growth (Fig. 5a and b). The columns are hexagonal in shape with  $\sim 200\text{ nm}$  in diameter and extend through the whole film thickness ( $5\text{--}6\text{ }\mu\text{m}$ ). The surfaces of the coldest samples were interspersed with cracks along the columns, which reach also through the whole layer thickness. From the differently shaped grains at the crack edges it appears that the cracks were formed already during the initial film nucleation and then grow along with the film. For higher substrate temperatures fewer cracks were observed.

The second growth mode ranges from  $350\text{ }^{\circ}\text{C}$  to  $460\text{ }^{\circ}\text{C}$ . The samples show pyramidally shaped grains. From the cross-section SEM pictures (Fig. 5c and d) it appears that the grains extend through the whole film thickness. The surface grain size linearly increases from  $\sim 0.5\text{ }\mu\text{m}$  at substrate temperatures of  $350\text{ }^{\circ}\text{C}$  to  $1.5\text{ }\mu\text{m}$  at  $460\text{ }^{\circ}\text{C}$ . Layers grown within this temperature region exhibit a high density of deep pinholes.

The third growth mode starts at a temperature of  $\sim 460\text{ }^{\circ}\text{C}$  and is characterized by irregularly shaped grains (Fig. 5e and f) and a high surface roughness as determined with AFM. The

grain size is non-uniformly distributed with very large grains ( $\sim 5\text{ }\mu\text{m}$ ) surrounded by smaller ones ( $\sim 1\text{ }\mu\text{m}$ ). The layers appear dense and compact. While the transition from the first growth mode to the second is very sharp, the transition from the second to the third is rather gradual.

#### 4. Discussion

The introduced growth regimes bear some resemblance to the Structure Zone Model (SZM) for thick sputtered films introduced by Thornton [10] and briefly summarized in the following. This SZM predicts three different structural zones and a transition zone as a function of  $T/T_m$ , where  $T$  is the substrate temperature and  $T_m$  the melting point of the film material. The first zone for  $T/T_m$  up to 0.3 consists of tapered or columnar crystals with open grain boundaries. The morphology of the layers in this zone results from zero surface diffusion and a unity condensation coefficient, which means that every atom sticks where it lands. The grains grow with the orientation of the initial nuclei. The transition zone (TZ) between zone I and II is defined as the limit of zone I for zero  $T/T_m$  and infinitely smooth substrate. In the TZ, the grains generally appear fibrous with a very small diameter and intimate contact between the grains. The surface structure and surface roughness is defined by the substrate grain size, -roughness and -impurities.

Zone II is observed for substrate temperatures  $0.3 < T/T_m < 0.5$  and is characterized by evolutionary growth due to adatom diffusion. The structure is often columnar and grains exhibit a near-equiaxed shape. In zones TZ and II the grain shape may be influenced by a growth rate, which depends on the surface energy of the different crystallographic planes. The film surface may then be dominated by the slow-growing surface planes.

Zone III is characterized by bulk diffusion processes such as recrystallization and grain growth for temperatures above  $T/T_m > 0.5$ . Grains appear equiaxed, dense and with shapes that do not coincide with substrate or film surface topography.

The first growth regime of the CdTe layers identified in this work shows similarities to the transition zone (TZ) and may therefore be governed by zero surface mobility and a unity sticking coefficient. The grain size and surface roughness is then determined by the substrate properties. This is also expressed by the lateral dimension of the columns, which equals the grain size of the CdS substrate. The orientation is given by the orientation of the initial nuclei, which are for bcc, fcc and hcp structures the most densely populated planes ((111) for cubic CdTe). The second growth regime may be equal to zone II. The grains have lost their relation to the substrate. But in contrast to the properties associated with zone II of the SZM, the CdTe layers in the second growth regime show a high density of pinholes. The loss in texture and the regaining of it for higher temperatures is also not included in the SZM. The third growth regime is comparable to zone III. The large and randomly orientated grains can be explained by re-crystallisation, re-nucleation and grain growth. However, this regime leads to large three dimensional crystallites.

## 5. Summary

CdTe-layers were deposited with CSS-technique on CSS-deposited CdS-substrates. The substrate temperature and source temperature have been varied. The growth rate has been plotted vs. the substrate temperature for different source temperatures. For a given source temperature two zones of growth rate were observed. Up to a substrate temperature of about 460 °C a constant growth rate, which depends on the source temperature, was measured. After a breaking point the growth rate decreases exponentially to zero.

XRD and SEM measurements have been performed to investigate the influences of deposition parameters on morphology. With both techniques three major regimes are identified. The first (substrate temperature below 350 °C) shows only (111) oriented grains and a strictly columnar grain

growth with a small grain size of about 200 nm, which seems to be defined by CdS-substrate. The second growth regime (substrate temperatures between 350 °C and 460 °C) is characterized by a preferred (111) texture but shows pyramidally shaped grains (with a grain size from 0.5–1.5 µm) with a high density of pinholes. The third regime coincides with the onset of decreasing growth rate. It is characterized by an almost statistical distribution of grain orientations with a slight preference for (220) and (311)-texture for very high temperatures. Very large grains (5–10 µm in diameter) exhibit irregular shapes and are surrounded by smaller grains. So far the best solar cells with a maximum conversion efficiency of 9.7% have been obtained in the lower temperature region of the third growth regime.

Further investigations are planned to show correlations between layer-morphology and electrical properties and to identify the basic mechanisms leading to the different growth regimes and possible routes to control the film morphology and resulting efficiencies.

## Acknowledgement

This work was supported by the German Federal Environment Ministry (grant no. 0329857A: “High Efficiency CdTe Thin Film Solar Cells”).

## References

- [1] X. Wu, *Solar Energy* 77 (6) (2004) 803.
- [2] A.W. Brinkmann, *Properties of Narrow Gap Cadmium-Based Compounds*, Ed. P. Capper, *Electronic Materials Information Services*, vol. 10, IEE, London, 1994, p. 591.
- [3] R.H. Bube, *Photovoltaic Materials*, Imperial College Press, London, 1998.
- [4] M. Burgelman, S. Degraeve, P. Nollet, *Appl. Phys. A* 63 (1999) 149.
- [5] J.H. Lee, *Jpn. J. Appl. Phys.* 40 (2001) 6741.
- [6] S.N. Alamri, *Phys. Status Solidi, A Appl. Res.* 200 (2) (2003) 352.
- [7] V.D. Falcão, *Mater. Res.* 9 (1) (2006) 29.
- [8] J. Fritsche, A. Klein, W. Jaegermann, *Adv. Eng. Mater.* 7 (2005) 914.
- [9] G.B. Harris, *Philos Mag.* 43 (1952) 113.
- [10] J.A. Thornton, *Ann. Rev. Mater. Sci.* 7 (1977) 239.